23rd ABCM International Congress of Mechanical Engineering
December 6-11, 2015, Rio de Janeiro, RJ, Brazil

MIXED CONVECTION STUDY IN A VENTILATED SQUARE CAVITY USING NANOFLUIDS

Paulo Mohallem Guimarães
Universidade Federal de Itajubá - Campus Itabira
Rua Irmã Ivone Drumond, 200, Distrito Insdustrial II, 35903-087, Itabira, MG - Brasil
e-mail: pauloguimaraes@unifei.edu.br

Renato José Pinto
rjpinto@fei.edu.br
Genésio José Menon
genesio@unifei.edu.br
Universidade Federal de Itajubá - Campus Itajubá
Av. BPS, 1303, Pinheirinho, 375000903, Itajubá, MG - Brasil

***Abstract**. This work aims to study the heat transfer mixed convection in a square cavity with openings on the vertical walls through which nanofluid flows. The intention is to cool a square heat source placed at the center of the geometry. The nanofluid has Copper nanoparticles and water as its base-fluid. The velocity and temperature of the entrance flow are known. A FORTRAN code is used to simulate the problem using the finite element method. The flow regime is laminar and transient. Some results are validated with experimental as well as numerical works. Then, a mesh independency study is carried out to look for an appropriate mesh that offers a tolerance deviation on the Nusselt number and the maximum temperature on the surface of the heat source. Some parameters are ranged as follows: i) the Reynolds number from 50 to 500, the nanofluid volume fraction Ø from 0 to 1%, the Grashof number from 10^3 to 10^5.*

***Keywords:** Nanofluid, Mixed Convection, Finite Element Method*

1. INTRODUCTION

The study of nanofluid behavior in engineering problems has had an enormous advance in recent years due to computational increasing power, not only in what deals with more powerful machines, but also in techniques and in commercial software in numerical simulation. Furthermore, nanofluid appearance in order to enhance heat transfer has significantly been successful and has been given special attention by the scientific family in some areas such as: i) heat exchangers; ii) medicine transport inside human body, electronic components, solar collectors and so on and so forth. A feature of the present study is to use nanofluid as the refrigerant fluid in order to cool a heat source that can be extended to a certain heat exchanger once one may see symmetry in the cavity where isolation boundary conditions are applied.

Shahi et al. (2010) investigated the mixed convection flows through a copper-water nanofluid in a square cavity with inlet and outlet ports. Buoyancy forces were that feature natural convection were attained by heating from the constant flux heat source located at the bottom wall and by cooling from the inlet flow. The governing equations were approximated by using the finite volume approach, using SIMPLE algorithm on the collocated arrangement. The study was carried out for the Reynolds number raging from 50 to 1000, with Richardson numbers from 0 to 10. The nanoparticle concentration was ranged from 0 to 0.05. The thermal conductivity and effective viscosity of nanofluid were calculated by Patel and Brinkman (1952) models, respectively. Results were presented in the form of streamlines, isotherms, average Nusselt number and average bulk temperature. In addition, the effects of solid volume fraction of nanofluids on the hydrodynamic and thermal characteristics were studied. The results indicated that increase in solid concentration led to increase in the average Nusselt number at the heat source surface and to decrease in the average bulk temperature.

Nassan et al. (2010) investigated the heat transfer in a square cross-section cupric duct in laminar flow under uniform heat flux by comparing heat exchange characteristics of Al_2O_3/water and CuO/water nanofluids. Sometimes because of pressure drop limitations, the need for noncircular ducts appeared and a testing facility was constructed for this purpose. Experimental studies were carried out being that those nanofluids had different nanoparticle concentrations. Distilled water was the base fluid to compose the nanofluids. The results showed that a significant heat transfer enhancement was achieved by both nanofluids compared with the case when pure water was used as the work fluid. Nevertheless, nanofluid with monoxide of copper showed better heat transfer augmentation compared with nanofluid with alumina through the square cross-section duct.

Rostamani et al. (2010) studied the turbulent flow of nanofluids with different volume concentrations of nanoparticles flowing through a two-dimensional duct under constant heat flux condition using numerical procedures. The nanofluids considered are mixtures of copper oxide (CuO), alumina (Al_2O_3) and oxide titanium (TiO_2) nanoparticles and water as the base fluid. All the thermophysical properties of nanofluids are temperature-dependent. The viscosity of nanofluids is obtained on basis of experimental data. The predicted Nusselt numbers exhibit good agreement with Gnielinski's correlation. The results show that by increasing the volume concentration, the wall shear stress and heat transfer rates increase. For a constant volume concentration and Reynolds number, the effect of CuO nanoparticles to enhance the Nusselt number is better than Al_2O_3 and TiO_2 nanoparticles.

Jung et al. (2009) studied the nanofluid convective heat transfer coefficient and friction factor behavior in rectangular microchannels. A microsystem consisting of a single microchannel on one side, and two localized heaters and five polysilicon temperature sensors along the channel on the other side were fabricated. Aluminum dioxide (Al_2O_3) with diameter of 170 nm nanofluids with various particle volume fractions were used. The convective heat transfer coefficient of the Al_2O_3 nanofluid in laminar flow regime was measured to be increased up to 32% compared to the distilled water at a volume fraction of 1.8 volume percent without major friction loss. The Nusselt number increased as Reynolds number went up in laminar flow regime. The Nusselt number, which was less than 0.5, was successfully correlated with Reynolds number and Prandtl number based on the thermal conductivity of nanofluids.

2. PROBLEM

The goal of the present work is to study numerically the laminar mixed convection inside a square ventilated cavity with a square heat source. The flow is ascending or descending when enters the lower part and exits the upper part of the vertical walls of the cavity or the opposite, respectively, that is, it leaves the lower part and enters in the upper part of the vertical walls of the cavity All walls are thermally isolated and have no-slip condition. The heat source has a constant and uniform heat flux. The nanofluid is composed of water (base-fluid and Prandtl number Pr = 6.2) and copper nanoparticles. The nanofluid enters the cavity at constant velocity and low temperature and exits under symmetry conditions related to the Y-direction. The nanoparticle concentration (Ø) is 1% due to the thermophysical property correlations applied here. Figure 1 depicts the problem geometry and boundary conditions. U and V are the dimensionless velocities, W is the cavity width, H is the cavity height, θ is the dimensionless temperature, and ρnf, μnf, and k_{nf} are the density, absolute viscosity and thermal conductivity of the nanofluid, respectively. These dimensionless variables and thermophysical parameters are going to be formally introduced later on.

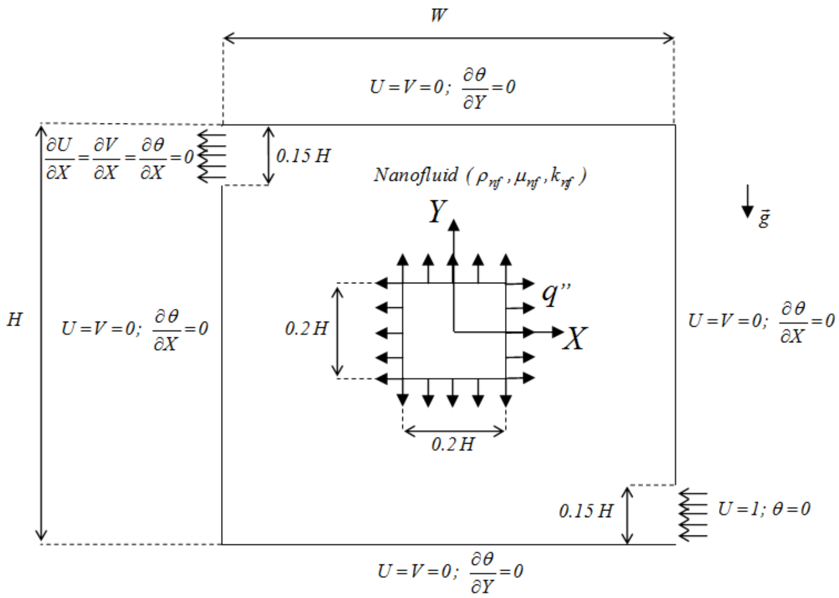

Figure 1. Geometry and boundary conditions only for the ascending flow

The dimensionless form of the conservation equations are:

$$\frac{\partial U}{\partial X}+\frac{\partial V}{\partial Y}=0 \qquad (1)$$

$$U\frac{\partial U}{\partial X}+V\frac{\partial U}{\partial Y}=-\frac{\partial P}{\partial X}+\frac{1}{Re}\frac{\mu_{eff}}{\nu_f\,\rho_{nf}}\left(\frac{\partial^2 U}{\partial X^2}+\frac{\partial^2 U}{\partial Y^2}\right) \tag{2}$$

$$U\frac{\partial V}{\partial X}+V\frac{\partial V}{\partial Y}=-\frac{\partial P}{\partial Y}+\frac{1}{Re}\frac{\mu_{eff}}{\nu_f\,\rho_{nf}}\left(\frac{\partial^2 V}{\partial X^2}+\frac{\partial^2 V}{\partial Y^2}\right)+\frac{(\rho\beta)_{nf}}{\rho_{nf}\,\beta_f}Ri\,\theta \tag{3}$$

$$U\frac{\partial \theta}{\partial X}+V\frac{\partial \theta}{\partial Y}=\frac{\alpha_{nf}}{\alpha f}\frac{1}{Pr\,Re}\left(\frac{\partial^2 \theta}{\partial X^2}+\frac{\partial^2 \theta}{\partial Y^2}\right) \tag{4}$$

where the nanofluid effective density ρ_{nf} and the nanofluid thermal difussivity α_{nf} are:

$$\rho_{nf}=(1-\phi)\,\rho_f+\phi\,\rho_p \tag{5}$$

$$\alpha_{nf}=k_{nf}\Big/\left(\rho C_p\right)_{nf} \tag{6}$$

and Ø is the solid volume fraction of the nanoparticles. The subscripts f and p stand for fluid and particles, respectively. The nanoparticle, which will be considered in this study, is Copper (Cu). The base fluid is water with Prandtl number (Pr) equal to 6.2. Table 1 gives the thermophysical properties of water and nanoparticles according to Oztop and Abu-Nada (2008):

The heat capacitance $(\rho Cp)_{nf}$ and the thermal expansion $(\rho\beta)_{nf}$ of the nanofluid are written as:

$$\left(\rho C_p\right)_{nf}=(1-\phi)\left(\rho C_p\right)_f+\phi\left(\rho C_p\right)_p \tag{7}$$

$$(\rho\beta)_{nf}=(1-\phi)(\rho\beta)_f+\phi(\rho\beta)_p \tag{8}$$

The effective dynamic viscosity μ_{nf} of the nanofluid (Brinkman (1952)) is:

$$\mu_{nf}=\frac{\mu_f}{(1-\phi)^{2.5}} \tag{9}$$

The thermal conductivity k_{nf} in Eq. (6), for spherical particles and based on Maxwell –Garnett's model (1904), is:

$$k_{nf}=k_f\left[\frac{\left(k_p+2k_f\right)-2\phi\left(k_f-k_p\right)}{\left(k_p+2k_f\right)+\phi\left(k_f-k_p\right)}\right] \tag{10}$$

where k_p is the thermal conductivity addressed to nanoparticle (Copper), and k_f is the thermal conductivity addressed to pure fluid (water). The Maxwell-Garnett's model has been cited by other authors such as Aminossadati and Ghasemi (2009), Ho et al. (2008) and Oztop and Abu-Nada (2008).

Table 1. Thermophysical properties of the nanoparticle and base-fluid.

Thermophysical properties	Fluid phase (water)	*Cu*
Cp (J/kgK)	4179	385
ρ (kg/m^3)	997.1	8933
K (W/mK)	0.613	400
β x 10^{-5} (1/K)	21	1.67

The dimensionless parameters are:

$$X=\frac{x}{H};Y=\frac{y}{H};U=\frac{u}{u_0};V=\frac{v}{u_0};P=\frac{p}{\rho_{nf}u_0};\theta=\frac{(T-T_c)}{(\Delta T)};\ Gr=\frac{g\beta_f H^3\Delta T}{{\nu_f}^2};\Delta T=\frac{q''H}{k_f};Pr=\frac{\nu_f}{\alpha_f};Ri=\frac{Gr}{Re^2};Re=\frac{u_o H}{\mu_f} \tag{11}$$

where: u and v – dimensional velocities, U and V – dimensionless velocities, p – dimensional pressure, P-dimensionless pressure, T – dimensional temperature, θ – dimensionless temperature, Gr – Grashof number, Pr – Prandtl number, Ri - Richardson number, ν – kinematics viscosity, α – thermal diffusivity, Re – Reynolds number.

The local Nusselt number on a certain surface is given by:

$$Nu^*_{hs}=\frac{hL}{k_f} \tag{12}$$

where *h* is the heat transfer coefficient:

$$h=\frac{q''}{T_s-T_c} \tag{13}$$

Substituting appropriate parameters from (11) and (17) into (16) yields the local Nusselt number:

$$Nu^*_{hs}(X,Y)=\left.\frac{1}{\theta(X,Y)}\right|_{hs} \tag{14}$$

where the subscript hs stands for the heater surface. Being that S is the surface length on where Nu^*_{hs} is integrated, the average Nusselt number is then calculated by:

$$Nu_{hs}(X,Y)=\frac{1}{S}\int_{hs}Nu^*_{hs} \tag{15}$$

3. NUMERICAL PROCEDURE AND CODE VALIDATION

Equations (1) to (4) are approximated by the finite element method with Petrov-Galerkin weighting on the convective terms and the pressure terms are approximated by a penalty technique with the penalty parameter equal to 10^9. These techniques will be omitted here for a space matter. The numerical method is implemented by using Fortran computational language. The code is thoroughly validated. However, just one is shown in Table 2 and it is related to nanofluid behavior. The problem is taken from Aminossadati and Ghasemi (2009). The problem consists of a square cavity with a heat source with length B placed on the middle of the bottom surface. All walls are cooled at temperature zero, but the remaining bottom surface, which is isolated. The base fluid is water with Pr = 6.2 and the nanoparticles used are Copper, Alumina and Titanium Oxide. Results for average Nusselt number and maximum temperature on the heat source are obtained for Ra equal 10^3, 10^4(not shown), 10^5(not shown) and 10^6. An excellent agreement is observed.

Table 2. Comparison for the case with a heater on the bottom of a square cavity with Ø = 0.1, B = 0.4 and Pr = 6.2.

		Nu_m		T_{max}	
		Present	Aminossadati and Ghasemi (2009)	Present	Aminossadati and Ghasemi (2009)
$Ra=10^3$	Cu	5.4681 (0.30%)	5.451	0.205 (0.00%)	0.205
	Al_2O_3	5.4075 (0.30%)	5.391	0.207 (0.00%)	0.207
	TiO_2	5.2058 (0.32%)	5.189	0.215 (0.00%)	0.215
$Ra=10^6$	Cu	13.5222 (2.53%)	13.864	0.109 (1.84%)	0.107
	Al_2O_3	13.4093 (1.89%)	13.663	0.110 (1.82%)	0.108
	TiO_2	13.1595 (1.95%)	13.416	0.113 (1.77%)	0.111

Two grids were studied. One with 34774 elements and the other with 51388 elements. A deviation of less than 1% was achieved. The grid with 51388 elements was adopted. The cases studied with these two grids are supposed to present results for extreme physical parameters such as Gr = 10^3 and Gr =10^5, and volume fraction 0 (pure water) and 0.01. A special attention is given to the elements adjacent to the wall on which the average Nusselt numbers on the heat source and cold wall, Nu_{hs} is going to be evaluated, since greater temperature gradients are expected there. The mesh quality is under the minimum angle of element internal angles, that is, elements are built by trying to set element angles as close as 90 degrees. The machine used to run all cases has 6Gb of RAM and processor Intel®Core™ 2 Duo CPU P7350 2Ghz. The convergence criterion to stop the program is:

$$Res = \frac{abs(Vel(\tau_i) - Vel(\tau_{i-1}))}{\Delta\tau} \leq 10^5 \tag{16}$$

where Res is the “largest velocity residual” in the entire domain in two consecutive time steps, that is:

$$\Delta\tau = \tau_i - \tau_{i-1} = 0.0005 \tag{17}$$

The velocity field lasts more than the temperature field to achieve convergence. This is why it is used in Eq. (16).

4. RESULTS

Figure 2 shows the isotherms and streamlines for Grashof numbers 10^3, 10^4, and 10^5, and Re = 50, 100, and 500, with nanoparticle concentration Ø equal to 1%. In general, for the cases just mentioned, there are flow recirculations. They are present near the inlet, in the right lower corner, and around the heat source. Recirculations may be brought about when the flow encounters a high pressure region and it must deviate from its path to another, practically contrary to the one the flow was following. Those high pressure regions may appear when one flow “blocks” the passage of another flow. This can be clearly illustrated in the cases where the forced velocities (primary flow) are predominant, that is, when Reynolds number is 500. The nanofluid that rises due to buoyancy forces and is also influenced by the adjacent primary flow does not have power enough to cross the primary flow and exits the cavity.

This creates secondary and also tertiary flows that are stuck around the heater and, therefore, creating an overheated region. One can observe from cases that go from left to right and from top to bottom in the table, the overheated flow region near the heat source goes from right to left on the top surface of the heated module. This is related to what extent the primary flow that starts from the inlet, goes towards the outlet by passing below the heat source, gets stronger. The stronger the primary flow is, the more difficult it is for the flow to cross that forced velocity path. Maybe, this is not the best layout to be followed. If the manufacturer of a heat exchanger has the opportunity to change the layout, maybe the one which brings forced convection downstairs against the ascending buoyancy forces may present a certain enhancement. But of course, this is some expectations and, hence, studies must be carried out to estimate any conclusion. Anyway, this is food for thought for future work. By keeping Grashof number constant (cases for Gr = 10^4 and 10^5), the temperature on the heat source surface increases when increasing the forced velocity at the inlet. Generally, one expects the heat transfer to increase when increasing Reynolds number. This happens almost in every paper we find in literature. However, here it is just proven that it may be not true. For Gr = 10^4, the maximum temperature goes from 0.240 to 0.3187 as Re is ranged from 50 to 500. Also, for Gr = 10^5, the maximum temperature goes from 0.2539 to 0.3045 for the same Re range. Thus, geometry together with boundary conditions may bring contradictions to what the reader is accustomed to face.

Figure 3 denotes the heat transfer behavior related to the ratio of inertia forces to viscous forces represented by the Reynolds number. For all cases, the heat transfer does not increase with Re due to reasons about which they were commented on previously in the isotherm and streamline figure section. Nevertheless, although the heat transfer enhancement is of low order, the nanoparticle concentration appears to increase heat transfer for Ø = 1%. This is not true for Gr = 10^4 and Re = 500. The high thermal conductivity of copper is expected to augment heat transfer; however more studies must be carried out to evaluate such case when Gr = 10^4 and Re = 500. As the method takes into consideration the Petrov-Galerkin method and the penalty formulation, it is suggested for next work that mass and energy conservation in the whole cavity, especially for that case, must be thoroughly analyzed.

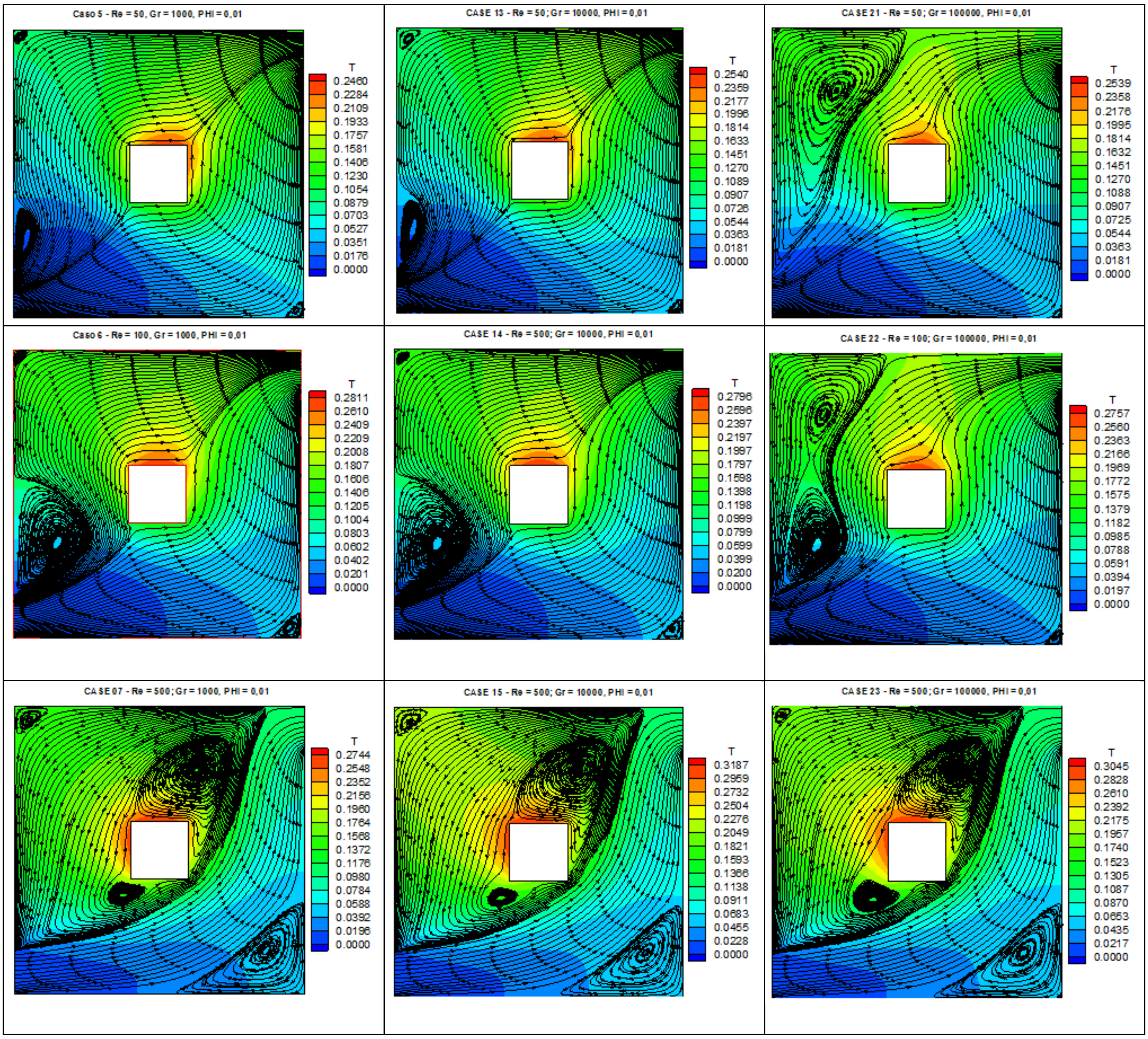

Figure 2. Isotherms and streamlines for cases with Gr = 10^3, 10^4, and 10^5, and Re = 50, 100, 500, Ø = 0.1

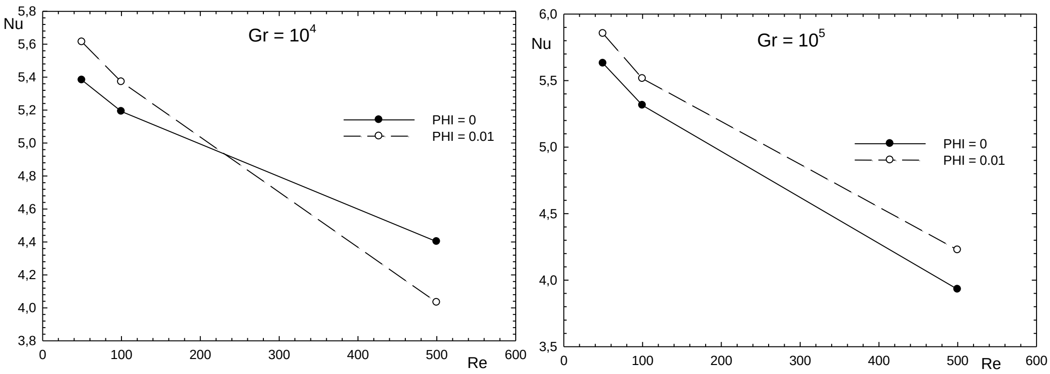

Figure 3. Nusselt versus Reynolds number for Gr = 10^4 and 10^5 for Ø = 0 and 1%

The results from now on will be about the cases with descending flow.

Figure 5 depicts isotherms and streamlines for Gr = 10^3 to 10^5, and Re = 50 to 500, volume fraction 0.1 when the forced convection is in the descending direction, that is, the cavity inlet is in the upper side and the cavity outlet is in the lower side of the geometry. Some behaviors are similar to those when considering the ascending forced convection. One can observe that here, flow stuck around the square heat source also happens, however, this occurs for almost every case shown in Figure 5. The primary flow passes over the heat source for the cases where Re are high (500) and the forced convection is more significant. In a general way, one may avoid using cases where the flow is stuck around the heat sources. In cases 45, 46 and 47, one can note the primary flow changing its position when taking the heat source as reference. In cases 45 and 46 the buoyancy forces are high enough to create an area of high pressures that are able to force the direction of the primary flow pass below the heat source. On the other hand, the flow for Re = 500 is sufficiently strong to break through that area and forces its way over the heat source.

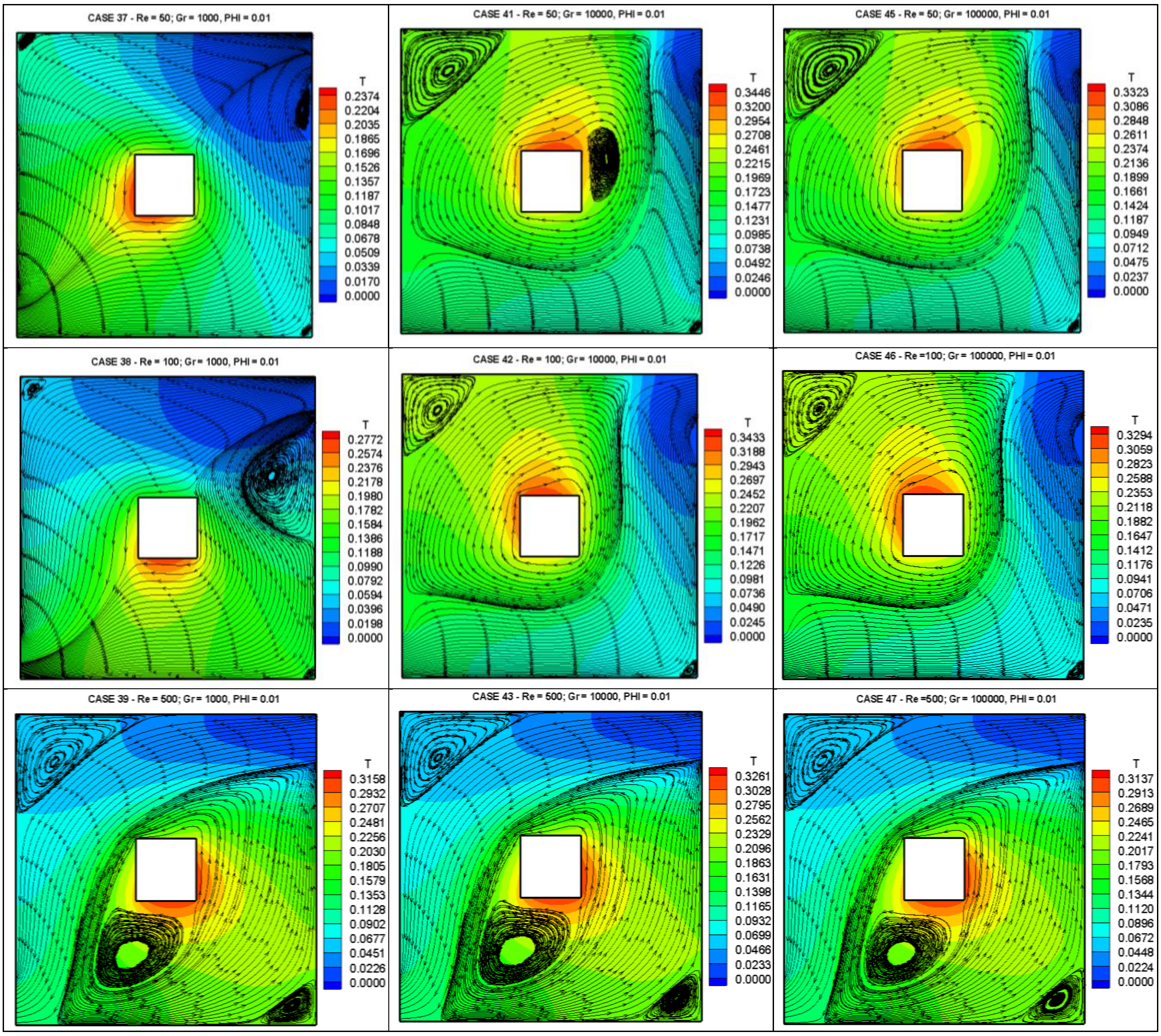

Figure 5. Isotherms and streamlines for cases with Gr = 10^3, 10^4, and 10^5, and Re = 50, 100, 500, Ø = 0.1

Figure 6 shows the average Nusselt number on the heat source versus Reynolds number for Gr = 10^3 and 10^5 and Ø equals 0 and 1%. There is an interesting at this point. For Gr = 10^3, Nu behaves quite the same as the corresponding cases in the ascending forced convection. Nevertheless, its behavior for Gr = 10^5 is totally contrary to its corresponding case in the ascending forced convection, that is, the Nusselt number tends to increase when increasing forced velocities. This probably due to the position change of the primary forced flow and the position change of the stuck recirculations around the heat source. These recirculation directions are the same, that is, both are counterclockwise, though.

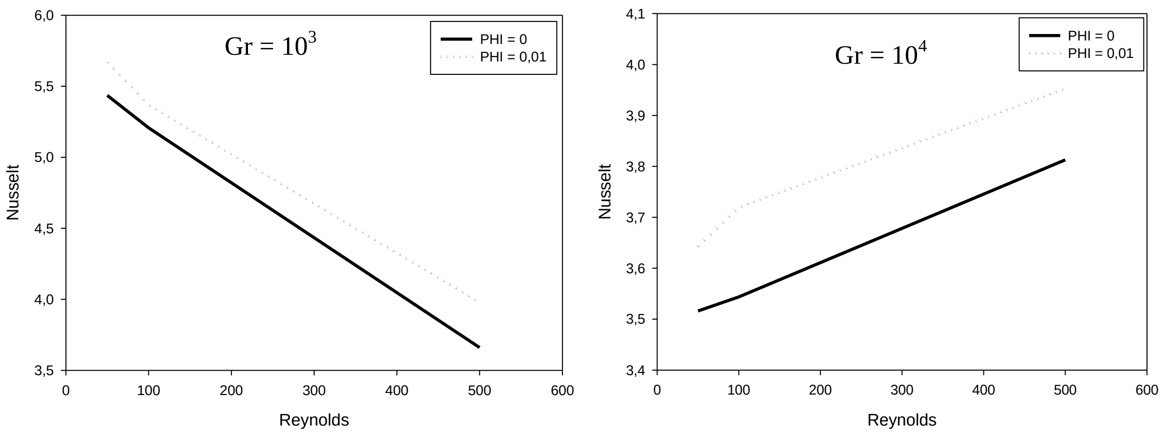

Figure 6. Nusselt versus Reynolds number for Gr = 10^3, 10^4 and 10^5 for Ø = 0 and 1%

5. ACKNOWLEDGEMENTS

The authors thank Fapemig (process code: APQ-02457-12).

6. REFERENCES

Aminossadati S. M., Ghasemi B., 2009. “Natural convection cooling of a localized heat source at the bottom of a nanofluid-filled enclosure”, *European Journal of Mechanics B/Fluids*, vol. 28, pp. 630-640.

Brinkman H. C., 1952. The viscosity of concentrated suspensions and solution”, *Journal of Chemical Physics*, vol. 20, pp. 571-581.

Ho C. J., Chen M. W., Li Z. W., 2008. “Numerical simulation of natural convection of nanofluid in a square enclosure: effects due to uncertainties of viscosity and thermal conductivity”, *International Journal of Heat and Mass Transfer*, vol. 51 (17-18), pp. 4506-4516

J. Jung, H. Oh, H. Kwak, 2009. “Forced convective heat transfer of nanofluids in microchannels, International Journal of Heat and Mass Transfer”, vol. 52, pp. 466-472.

Maxwell J., “A treatise on electricity and magnetism”, second ed. Oxford University Press, Cambridge, UK, 1904.

Nassan T. H., Heris S. Z., Noie S. H., 2010. “A comparison of experimental heat transfer characteristics for Al_2O_3/water and CuO/water nanofluids in square cross-section duc”, *International Communications of Heat and Mass Transfer*, vol. 37, pp. 924-928.

Oztop H. F., Abu-Nada E., 2008. “Numerical study of natural convection in partially heated rectangular enclosures filled with nanofluids”, *International Journal of Heat and Fluid Flow*, vol. 29 (5), pp. 1326-1336.

Rostamani M., Hosseinizadeh S. F., Gorji M., Khodadadi J. M., 2010. “Numerical study of turbulent forced convection flow of nanofluids in a long horizontal duct considering variable properties”, *International Communications in Heat and Mass Transfer*, vol. 37 (10), pp. 1426-1431.

Shahi M., Mahmoudi A. H., Talebi F., 2010. “Numerical study of mixed convective cooling in a square cavity ventilated and partially heated from the below utilizing nanofluid”, *International Communications in Heat and Mass Transfer*, vol. 37, pp. 201-213.

7. RESPONSIBILITY NOTICE

The authors are the only responsible for the printed material included in this paper.